

Article

Adsorption Affinities of Small Volatile Organic Molecules on Graphene Surfaces for Novel Nanofiller Design: A DFT Study

Francesco Moriggi , Vincenzina Barbera , Maurizio Galimberti *  and Giuseppina Raffaini * 

Department of Chemistry, Materials, and Chemical Engineering “Giulio Natta”, Politecnico di Milano, via Luigi Mancinelli 7, 20131 Milano, Italy; francesco.moriggi@polimi.it (F.M.); vincenzina.barbera@polimi.it (V.B.)
* Correspondence: maurizio.galimberti@polimi.it (M.G.); giuseppina.raffaini@polimi.it (G.R.)

Abstract: The adsorption of organic molecules on graphene surfaces is a crucial process in many different research areas. Nano-sized carbon allotropes, such as graphene and carbon nanotubes, have shown promise as fillers due to their exceptional properties, including their large surface area, thermal and electrical conductivity, and potential for weight reduction. Surface modification methods, such as the “pyrrole methodology”, have been explored to tailor the properties of carbon allotropes. In this theoretical work, an ab initio study based on Density Functional Theory is performed to investigate the adsorption process of small volatile organic molecules (such as pyrrole derivatives) on graphene surface. The effects of substituents, and different molecular species are examined to determine the influence of the aromatic ring or the substituent of pyrrole’s aromatic ring on the adsorption energy. The number of atoms and presence of π electrons significantly influence the corresponding adsorption energy. Interestingly, pyrroles and cyclopentadienes are 10 kJ mol^{-1} more stable than the corresponding unsaturated ones. Pyrrole oxidized derivatives display more favorable supramolecular interactions with graphene surface. Intermolecular interactions affect the first step of the adsorption process and are important to better understand possible surface modifications for carbon allotropes and to design novel nanofillers in polymer composites.

Keywords: adsorption; surface modification; DFT; nano-sized carbon allotropes; graphene; carbon nanotubes; supramolecular interactions; pyrrole methodology



Citation: Moriggi, F.; Barbera, V.; Galimberti, M.; Raffaini, G. Adsorption Affinities of Small Volatile Organic Molecules on Graphene Surfaces for Novel Nanofiller Design: A DFT Study. *Molecules* **2023**, *28*, 7633. <https://doi.org/10.3390/molecules28227633>

Academic Editor: Erich A. Müller

Received: 7 October 2023

Revised: 6 November 2023

Accepted: 10 November 2023

Published: 16 November 2023



Copyright: © 2023 by the authors. Licensee MDPI, Basel, Switzerland. This article is an open access article distributed under the terms and conditions of the Creative Commons Attribution (CC BY) license (<https://creativecommons.org/licenses/by/4.0/>).

1. Introduction

The adsorption process on solid surfaces plays a critical role in numerous scientific disciplines, ranging from chemistry and physics to materials science and nanotechnology [1–8]. Many phenomena can occur when molecules adsorb on solid surface. The ability to understand and manipulate the interactions between molecules and surfaces opens up avenues for designing novel materials with tailored surface properties and optimizing the performance of existing systems [9–15]. While experimental techniques provide valuable information about surface adsorption, a deeper understanding at the atomic level requires the use of numerical simulations that can help us study the possible mechanisms and dynamics driving these processes [16–22].

Density Functional Theory (DFT) calculations together with molecular mechanics (MM) and molecular dynamics (MD) methods can provide information that strongly complements experimental studies [23–38]. MM and MD simulations are interesting tools to describe both the bulk and surface properties of materials at the atomistic level [39–47]. The adsorption process of proteins, peptides, and small molecules can be investigated on the external surfaces of graphite and carbon allotropes in general. The comparisons between theoretical results and experimental data are interesting, such as those concerning favorable van der Waals interactions between graphene allotropes and proteins, an important aspect for biomaterials in contact with the blood [43]. The same favorable interactions explain the possible solubilization of carbon nanotubes synthesized in an amorphous phase due to

protein adsorption on the external surface. Their solubilization is an important technology aspect to prepare aligned fibers in polymeric matrices of composite materials [47–49].

Considering the adsorption of a single molecule on a solid surface, Density Functional Theory has emerged as an interesting tool for studying the ground-state properties of condensed matter systems, particularly with regard to how surface interactions influence the electronic distribution in the molecular orbitals of the volatile organic molecules near a solid surface [50–53]. DFT offers a rigorous framework based on quantum mechanics, enabling accurate predictions of adsorption sites, binding energies, and electronic properties that closely align with experimental observations, allowing researchers to gain insights into the structural, electronic, and energetic aspects of adsorption, thus helping to clarify the fundamental principles that govern these phenomena [23,50–54].

In recent years, there has been a growing interest in surface modification techniques aiming to improve the properties of fillers used in advanced technological applications [55]. One prominent area where surface modification has shown significant potential is in the development of polymer composites for the tire industry [56–58]. By modifying the surfaces of fillers, scientists can achieve substantial improvements in mechanical strength, thermal stability, electrical conductivity, and other desired characteristics, thereby pushing the boundaries of material performance [59–62]. In this context, nano-sized carbon allotropes, such as graphene and carbon nanotubes, have emerged as promising candidates due to their exceptional properties [63,64]. Carbon allotropes display a remarkable combination of attributes that make them highly attractive as fillers in polymer composites [65–71]. Their large surface area provides an extended contact interface with the surrounding polymer matrix, enabling efficient load transfer and reinforcing the mechanical properties of the composite [66–68]. Additionally, carbon allotropes exhibit exceptional thermal and electrical conductivity, facilitating heat dissipation and electrical conduction pathways within the material. Furthermore, their incorporation into composites allows for a reduction in the volume ratio of fillers compared to traditional alternatives, which can lead to lighter and more cost-effective materials [53]. Given these advantages, tailoring the properties of carbon allotropes has become a topic of considerable scientific interest, driving the exploration of various surface modification methods [69–74].

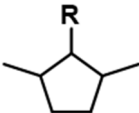
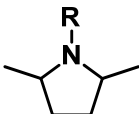
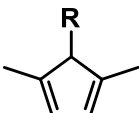
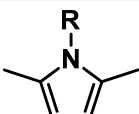
Among the diverse approaches investigated, one particularly efficient and reliable procedure is known as the “pyrrole methodology”, which involves the covalent modification of carbon allotrope surfaces using *N*-substituted pyrrole molecules [75,76], a method that enables the introduction of desirable functionalities onto the carbon allotrope surface. The grafting process begins with the initial adsorption of *N*-substituted pyrrole molecules onto the sp^2 carbon surface, which then undergoes oxidation and subsequent Diels–Alder cycloaddition, forming covalent bonds with the edges of the carbon allotrope plane. The adsorption and grafting mechanisms of the pyrrole methodology are governed by a complex interplay of supramolecular interactions, which dictate the stability, structure, and properties of the modified surface [77]. This approach has been employed to produce novel fillers in order to improve the mechanical properties of polymer nanocomposites [78,79].

Motivated by the potential of the pyrrole methodology and the need for a detailed understanding of the adsorption process, our study employed *ab initio* simulations based on DFT to gain deeper insights into the initial steps of the pyrrole methodology and investigate the adsorption behaviors of various compounds on carbon allotropes. Our objectives encompassed not only determining the optimal computational parameters for the simulations but also exploring the interactions between pyrrole molecules and graphene surfaces. Furthermore, we sought to examine the effects of substituents and oxidation on the adsorption process, allowing us to understand how different modifications influence the stability and reactivity of this system.

To broaden the scope of our investigation, we expanded our calculations to include other compounds, including alkanes, cyclopentanes, pyrrolidines, and cyclopentadiene derivatives. By exploring a broad range of molecular species, we aimed to uncover the underlying factors governing adsorption and shed light on the role of dispersion and π -

π interactions in stabilizing these systems on graphene surfaces, an approach that has already been verified in the recent literature [80–83]. The structures of the systems were studied by calculating their adsorption energies and generating charge difference density plots. These detailed analyses allowed us to obtain a comprehensive understanding of the supramolecular interactions at play and their influence on the adsorption phenomena occurring on carbon allotrope surfaces. Table 1 shows a list of the compounds adsorbed on the pristine graphene samples studied. The pyrrole compounds used to develop the “pyrrole methodology” were obtained from the Paal Knorr reaction [84,85] of a primary amine with 2,5-hexanedione (HD). This synthetic pathway gave the chance to start from a biobased chemical. Indeed, HD was prepared through the ring opening reaction of 2,5-dimethylfuran, also by using a two-step one pot process [86,87]. The use of HD led to pyrrole molecules with two methyl groups in the alpha positions of the ring. In Section 2.4, theoretical results about 1,2,5-trimethylpyrrole and its oxidized derivatives on a pristine graphene surface will be discussed. The use as reinforcing fillers of sp^2 carbon allotropes, mainly carbon black, functionalized by means of the “pyrrole methodology” with pyrrole compounds as the ones studied in the research here reported, improved the properties of elastomeric composites for a large-scale application such as the one in tyre compounds [87,88]. The development on an industrial scale was announced by a major player in the tyre field [89]. This study is aimed at giving a contribution to the development of the “pyrrole methodology”, elucidating its first step.

Table 1. A list of the studied compounds adsorbed on pristine graphene.

Compound	Structure Type	Structure
Alkane	Linear	H–R
Cyclopentane	Saturated cyclic	
Pyrrolidine		
Cyclopentadiene	Unsaturated cyclic	
Pyrrole		

2. Results and Discussion

In this section, the results about the adsorption of the different aliphatic and aromatic compounds reported in Table 1 on the pristine graphite surface are reported and discussed.

2.1. Adsorption of Linear Alkanes on the Pristine Graphene Surface

As described in the Materials and Methods section, linear alkane compounds such as methane, ethane, propane, and butane were considered close to the pristine surface of graphene. The optimized structures are shown to the left of all four panels in Figure 1, while the adsorption distances and adsorption energies are listed in Table 2. As seen in the latter, the adsorption distances ranged from 3.46 Å (methane) to 3.65 Å (ethane), and the adsorption energies increased with increasing carbon atoms in the alkyl chain, indicating

increased supramolecular interactions due to the forces of dispersion between the molecule and the graphene surface.

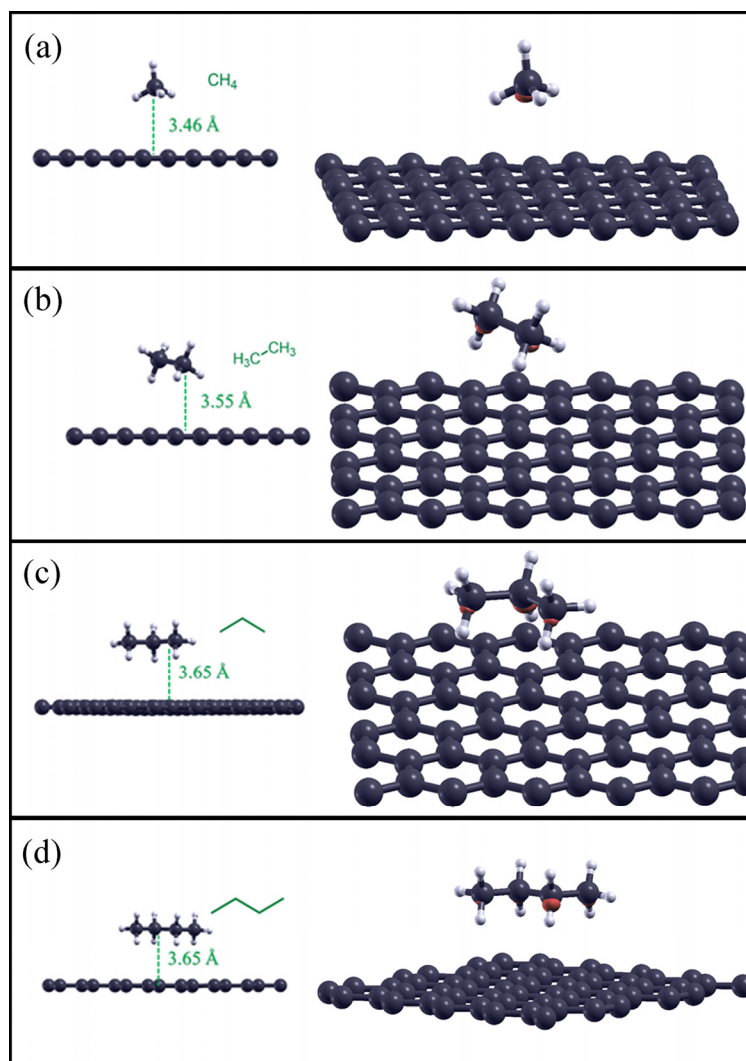


Figure 1. Optimized structures for the studied alkanes adsorbed on the pristine graphene surface (on the left), and their charge density difference plots (iso-surface value: 0.0003) on the surface (on the right). Methane adsorbed on graphene is reported in panel (a), ethane in panel (b), propane in panel (c), butane in panel (d), respectively.

Table 2. Adsorption distances and energies for alkane compounds adsorbed on the pristine graphene surface.

Compound	Distance, d (Å)	E_{ads} (kJ mol ⁻¹)
Methane	3.46	-13.2
Ethane	3.55	-18.7
Propane	3.65	-25.6
Butane	3.65	-32.7

The charge density difference iso-surfaces (value = 0.0003) shown to the right of all four panels in Figure 1 indicate the regions where there is charge transfer, and this information is useful for representing the nature of bonding between the elements present in the simulation. The small red clouds present for all adsorbents indicate a slight increase in charge density (charge per unit volume) pointing toward the graphene surface in the

direction of the C–H bond. The red clouds are more evident for propane and butane in Figure 1c,d, respectively.

Regarding the ground-state geometries studied, upon considering the plane defined by all carbon atoms in the propane and butane chains, it can be gleaned that this plane is parallel to the graphene plane. As regards the interaction energy, we can observe that as the number of carbon atoms in the chain increases, the interactions with the solid surface increase proportionally, indicating a stabilizing effect due, as mentioned previously, to the favorable dispersion interactions between the C–H bonds and the graphene surface.

2.2. Adsorption of Saturated Cyclic Compounds on the Pristine Graphene Surface

The results relating to the saturated cyclic systems reported in Table 1 are presented and discussed in this section, considering both cyclopentane and pyrrolidine compounds.

2.2.1. Adsorption of Cyclopentane Compounds on the Pristine Graphene Surface

As described in the Materials and Methods section, cyclopentane compounds were considered adsorbed on the pristine graphene surface. The ground-state structures are shown on the left in Figure 2, while the adsorption distances and the adsorption energies are reported in Table 3.

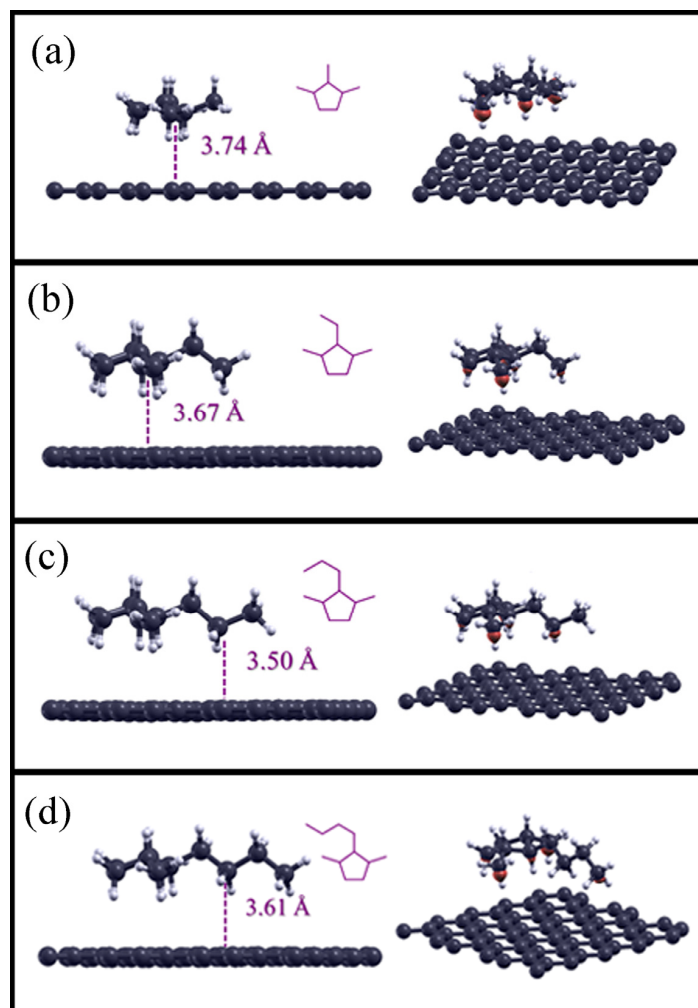


Figure 2. Optimized structures for the cyclopentane compounds adsorbed on the pristine graphene surface (on the left), and the charge density difference plots (iso-surface value: 0.0003) of the alkane compounds on the surface (on the right). 1,2,3-trimethylcyclopentane adsorbed on graphene is reported in panel (a), 2-ethyl-1,3-dimethylcyclopentane in panel (b), 2-propyl-1,3-dimethylcyclopentane in panel (c), 2-butyl-1,3-dimethylcyclopentane in panel (d), respectively.

Table 3. Adsorption distances and energies for cyclopentane compounds adsorbed on the pristine graphene surface.

Compound	Distance, d (Å)	E_{ads} (kJ mol ⁻¹)
1,2,3-trimethylcyclopentane	3.74	-48.1
2-ethyl-1,3-dimethylcyclopentane	3.67	-53.2
2-propyl-1,3-dimethylcyclopentane	3.50	-58.5
2-butyl-1,3-dimethylcyclopentane	3.61	-64.1

Compared to the previous results, considering the structures in the ground-state ranging from 1,2,3-trimethylcyclopentane to 2-butyl-1,3-dimethylcyclopentane, we observed a different arrangement of the structure of the alkyl residue -R with respect to the graphene plane: in fact, if we also consider for these structures the plane defined only by the carbon atoms linked to carbon 2 of the cyclopentane, this plane is now arranged perpendicular to the graphene surface, as reported in the panels on the left of Figure 2. The distances of carbon atoms closer to the graphene surface varied from 3.74 Å in 1,2,3-trimethylcyclopentane to 3.50 Å in 2-propyl-1,3-dimethylcyclopentane.

Concerning the strength of the interactions, the adsorption energies were higher when increasing the carbon atoms in linear chain, indicating, as with the alkane compounds, increased supramolecular interactions due to dispersion forces between these cyclopentane derivatives and the graphene surface.

Regarding the charge difference density plots (iso-surface value: 0.0003) shown on the right in all panels in Figure 2, and regarding the linear alkanes, the red clouds present for all the adsorbates indicate an increase in charge density that points toward the graphene surface.

As mentioned previously, regarding the geometry of the interactions in the calculated ground state, the alkyl chains that start from the cyclopentane are perpendicular to the graphene surface, and the adsorbate atoms that are close to the latter seem to contribute more to the overall supramolecular interactions. Moreover, because cyclopentanes are sp^3 -hybridized, there are no planar geometry constraints; thus, the molecules, after adsorption, adjust themselves to maximize the interaction forces due to C–H bonds and the graphene surface.

2.2.2. Adsorption of Pyrrolidine Compounds on the Pristine Graphene Surface

As described in the Materials and Methods section, pyrrolidine derivatives adsorbed on the pristine graphene surface were studied. The lowest total energy structures are reported in the panels on the left in Figure 3, while the adsorption distances and their adsorption energies are listed in Table 4. Compared to the previous results, the calculated distances of pyrrolidine compounds in the calculated ground state were, on average, smaller, ranging from 3.46 Å to 3.58 Å for 1-propyl-2,5-dimethylpyrrolidine and 1-ethyl-2,5-dimethylpyrrolidine, respectively. Using the same methodologies for the analysis of the theoretical results, the adsorption energies were calculated, and their values were found to be lower, and therefore more stable in the system, for molecules with a greater number of carbon atoms, which were comparable in size to compounds of cyclopentane.

Considering the graphs of the charge density differences for the pyrrolidines (see the right side in all panels in Figure 3), one can see, as in the previous case, the positive (red) contribution to the charge transfer between the carbon atoms and the surface of graphene. Compared to saturated homoatomic systems (e.g., alkanes and cyclopentanes), however, the nitrogen atom appeared to deplete the graphene surface, as can be gleaned from the blue cloud under the pyrrolidine ring. This could be explained by the fact that nitrogen possesses a lone pair of electrons, which, in addition to the dispersion forces between the C–H bonds and the graphene surface, can interact with the graphene surface via a π -type bond.

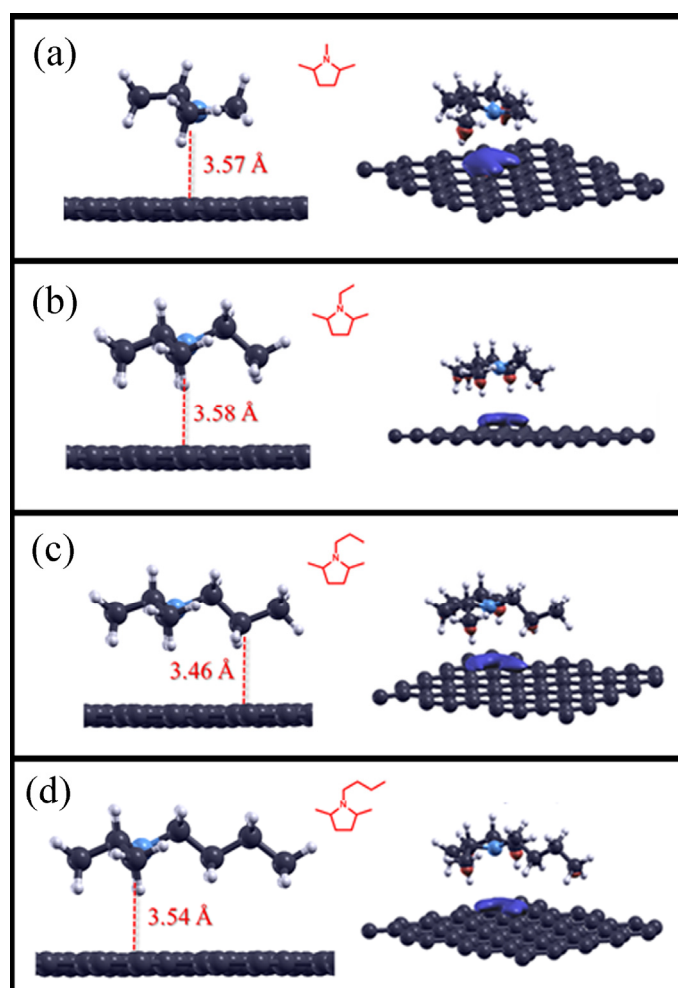


Figure 3. Optimized structures for pyrrolidine compounds adsorbed on the pristine graphene surface (on the left), and the charge density difference plots (iso-surface value: 0.0003) of alkane compounds on the surface (on the right). 1,2,5-trimethylpyrrolidine adsorbed on graphene is reported in panel (a), 1-ethyl-2,5-dimethylpyrrolidine in panel (b), 1-propyl-2,5-dimethylpyrrolidine in panel (c), 1-butyl-2,5-dimethylpyrrolidine in panel (d), respectively.

Table 4. Adsorption distances and energies for pyrrolidine compounds adsorbed on the pristine graphene surface.

Compound	Distance, d (Å)	E_{ads} (kJ mol ⁻¹)
1,2,5-trimethylpyrrolidine	3.57	−46.2
1-ethyl-2,5-dimethylpyrrolidine	3.58	−51.3
1-propyl-2,5-dimethylpyrrolidine	3.46	−56.5
1-butyl-2,5-dimethylpyrrolidine	3.54	−62.1

2.3. Adsorption of Unsaturated Cyclic Compounds on the Pristine Graphene Surface

The results regarding the unsaturated cyclic systems reported in Table 1 are presented and discussed in this section, considering both cyclopentadiene and pyrrole compounds.

2.3.1. Adsorption of Cyclopentadiene Compounds on Pristine Graphene Surface

As described in the Materials and Methods section, cyclopentadiene derivatives were adsorbed on the pristine graphene surface. The optimized structures are reported on the

left in all panels in Figure 4, while the adsorption distances and calculated adsorption energies are shown in Table 5.

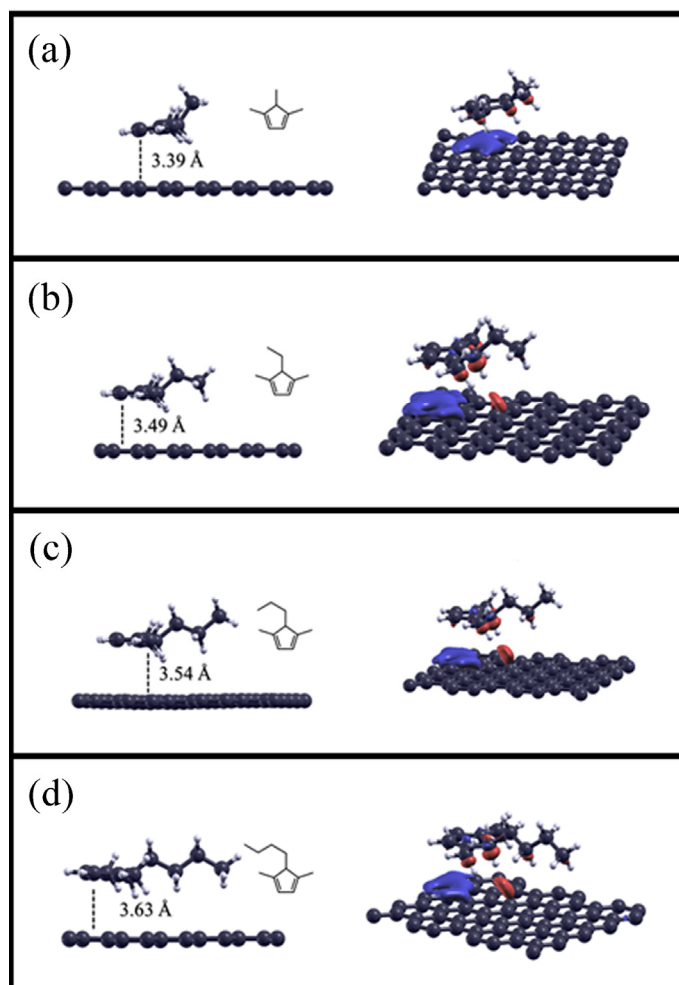


Figure 4. Optimized structures for cyclopentadiene compounds adsorbed on the pristine graphene surface (on the left), and the charge density difference plots (iso-surface value: 0.0003) of alkane compounds on the surface (on the right). 1,4,5-trimethylcyclopenta-1,3-diene adsorbed on graphene is reported in panel (a), 5-ethyl-1,4-dimethylcyclopenta-1,3-diene in panel (b), 5-propyl-1,4-dimethylcyclopenta-1,3-diene in panel (c), 5-butyl-1,4-dimethylcyclopenta-1,3-diene in panel (d), respectively.

Table 5. Adsorption distances and energies for cyclopentadiene compounds adsorbed on the pristine graphene surface.

Compound	Distance, d (Å)	E_{ads} (kJ mol ⁻¹)
1,4,5-trimethylcyclopenta-1,3-diene	3.57	−46.2
5-ethyl-1,4-dimethylcyclopenta-1,3-diene	3.58	−51.3
5-propyl-1,4-dimethylcyclopenta-1,3-diene	3.46	−56.5
5-butyl-1,4-dimethylcyclopenta-1,3-diene	3.54	−62.1

We can observe that the studied cyclopentadiene compounds, due to sp^2 hybridization, have a planar ring that is positioned parallel to the graphene surface to maximize the interaction area, with the distance d increasing as the number of atoms adsorbed increases.

Compared to the results for the previously reported saturated compounds, the calculated adsorption energies are higher but still follow the same trend, ranging from

$-51.5 \text{ kJ mol}^{-1}$ to $-67.7 \text{ kJ mol}^{-1}$ for 1,4,5-trimethylcyclopenta-1,3-diene and 5-butyl-1,4-dimethylcyclopenta-1,3-diene, respectively.

In the charge density difference plots shown in all panels on the right in Figure 4, we can observe that there are two contributions to the adsorption of cyclopentadiene derivatives on the graphene surface. Initially, dispersion interactions are significant, such as in alkane compounds, as indicated by the increase in charge density (red cloud) in the direction of the C–H bonds toward the graphene surface. Furthermore, the contribution of π interactions between the molecular π orbitals of the cyclopentadiene rings and the delocalized π orbitals of the graphene surface is important, highlighted in this case by the charge depletion (blue cloud) on the graphene surface.

2.3.2. Adsorption of Pyrrole Compounds on the Pristine Graphene Surface

As described in the Materials and Methods section, the theoretical results regarding the pyrrole derivatives adsorbed on the pristine graphene surface are shown and discussed in this section. The optimized structures can be seen in Figure 5, while the adsorption distances and calculated adsorption energies are listed in Table 6.

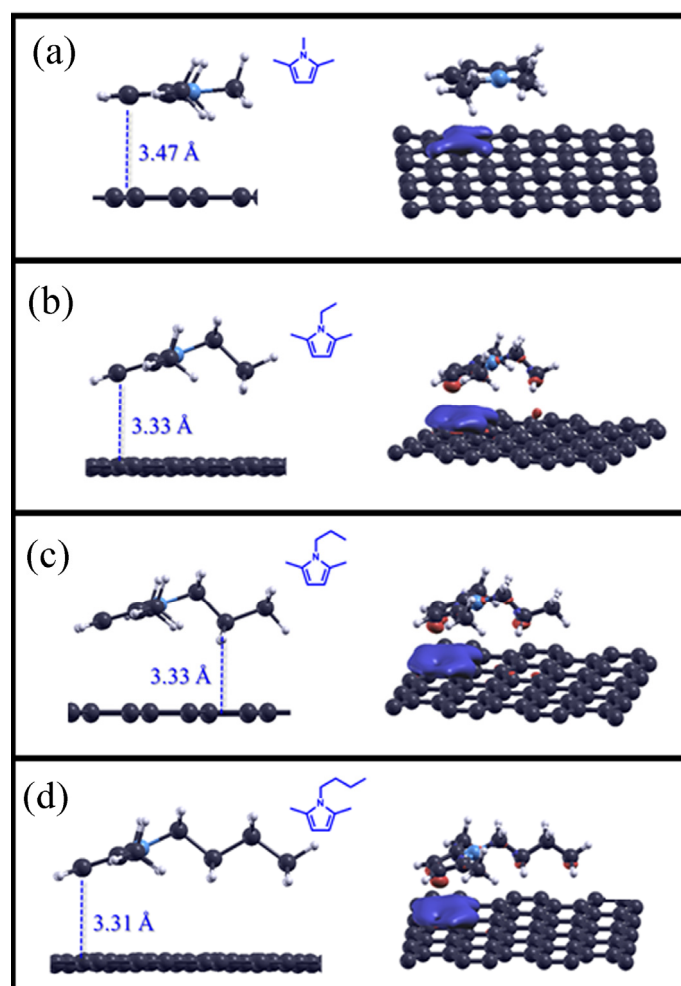


Figure 5. Optimized structures for pyrrole derivatives adsorbed on the pristine graphene surface (on the left), and the charge density difference plots (iso-surface value: 0.0003) of alkane compounds on the surface (on the right). 1,2,5-trimethylpyrrole adsorbed on graphene is reported in panel (a), 1-ethyl-2,5-dimethylpyrrole in panel (b), 1-propyl-2,5-dimethylpyrrole in panel (c), 1-butyl-2,5-dimethylpyrrole in panel (d), respectively.

Table 6. Adsorption distances and energies for pyrrole compounds adsorbed on the pristine graphene surface.

Compound	Distance, d (Å)	E_{ads} (kJ mol ⁻¹)
1,2,5-trimethylpyrrole	3.47	-55.3
1-ethyl-2,5-dimethylpyrrole	3.33	-54.9
1-propyl-2,5-dimethylpyrrole	3.33	-61.0
1-butyl-2,5-dimethylpyrrole	3.31	-66.3

Unlike unsaturated cyclopentadiene compounds, pyrroles are aromatic compounds, so the delocalized molecular orbitals in the ring constraint fix the carbon attached to the nitrogen in the same plane. This causes molecules that have a longer chain than that of 1,2,5-trimethylpyrrole to be slightly inclined and not perfectly parallel to the graphene surface, thus resulting in shorter adsorption distances between the molecule and the latter.

Even for these systems, the adsorption energy (E_{ads}) increases as the number of atoms in the molecule increases, specifically in the substituent of the linear alkyl chain, with values ranging from -55.4 kJ mol⁻¹ to -66.3 kJ mol⁻¹ for 1,2,5-trimethylpyrrole and 1-butyl-2,5-dimethylpyrrole, respectively.

In the graphs of the charge density differences reported on the right-hand panels in Figure 5 (iso-surface values: 0.0003), specifically regarding the cyclopentadiene derivatives, we can observe that two different contributions to the adsorption strength are important: the first contribution increases the density of charge between carbon atoms facing the direction of the C-H bond due to dispersion interactions, and the second contribution induces a charge depletion on the graphene surface due to π - π interactions.

In Figure 6, the adsorption energy on the pristine graphene surface has been plotted as a function of the number of atoms in the studied molecule. As expected, a linear correlation was found when increasing the number of carbon atoms present (see Table 7). Since there are no covalent or ionic bonds present between the molecule and the carbon substrate, the only forces exerted between these two systems are, as previously mentioned, due partly to dispersion and partly, if present in the case of adsorbates with free electron bonds in p-type orbitals, to π - π interactions. Further theoretical studies based on molecular mechanics and dynamics method on the role of the van der Waals contributions using a simulation previously proposed protocol [90] are an ongoing work.

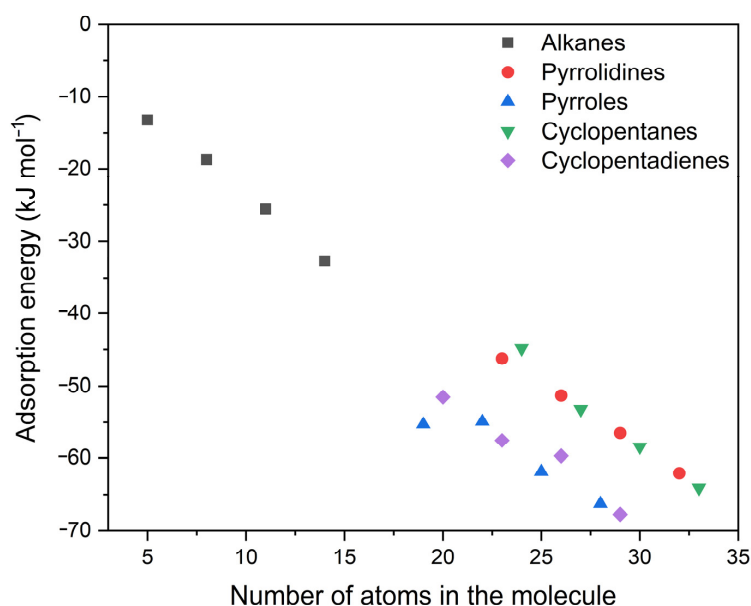
**Figure 6.** Adsorption energies of compounds adsorbed on the pristine graphene surface as a function of the number of atoms in the specific organic molecule.

Table 7. Information on the best linear fit with intercept equal to zero passing through the data related to the adsorption energy as a function of the number of atoms in the single molecules studied reported in Figure 6.

Compound	Slope	Standard Error	R^2
Alkanes	−2.3522	0.0426	0.9990
Pyrrolidines	−1.9616	0.0142	0.9998
Pyrroles	−2.5122	0.1050	0.9948
Cyclopentanes	−1.9371	0.0194	0.9997
Cyclopentadienes	−2.4005	0.0624	0.9980

For alkane and cyclopentane compounds, which lack these mechanisms, a possible adsorption mode is through the dispersion bond, while pyrrolidines, cyclopentadienes, and pyrroles, which have π electrons, can interact with the surface through π – π interactions. At the same number of atoms, cyclopentadiene and pyrrole compounds showed better stability and a gain of about 10 kJ mol^{-1} compared to their saturated counterparts, cyclopentanes and pyrrolidines, respectively. Interestingly, the pyrrole compounds, which interact better with the graphene surface, show a negative and greater slope in the best linear fit as reported in Table 7.

2.4. Adsorption of 1,2,5-Trimethylpyrrole and Its Oxidized Derivatives on Pristine Graphene Surface

To study the effect of oxidation, which, as described in the introduction, is a key step for the cycloaddition of pyrrole molecules onto carbon allotropes [77,91], 1,2,5-trimethylpyrrole and its oxidized derivatives were adsorbed on the pristine graphene surfaces and their adsorption energies calculated. In Figure 7, ground-state energy structures for TMP, TMP-CHO, and TMP-2CHO can be seen. For all the compounds, the value of the adsorption distance was found to be 3.46 \AA . Figure 8 shows the adsorption energies as a function of the number of carbon atoms in the organic adsorbates. As can be seen from the E_{ads} values, the presence of an aldehyde group favors the adsorption process, with a decrease of about 3 kJ mol^{-1} per aldehyde. This means that the oxidation of pyrrole compounds enhances the supramolecular interactions between the latter and the graphene surface, as the oxygen increases the number of π interactions with the conjugated graphene system. Regarding the effect of oxidation, we can conclude that the presence of aldehyde groups improved the adsorption energy for 1,2,5-trimethylpyrrole on the pristine graphene surface.

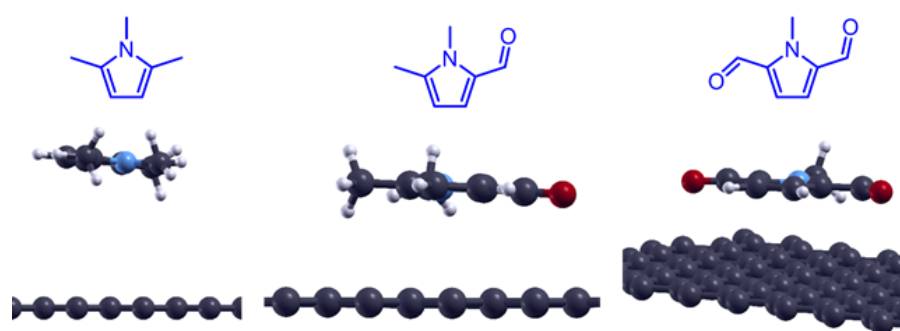


Figure 7. Optimized structures for TMP, TMP-CHO, and TMP-2CHO adsorbed on the pristine graphene surface.

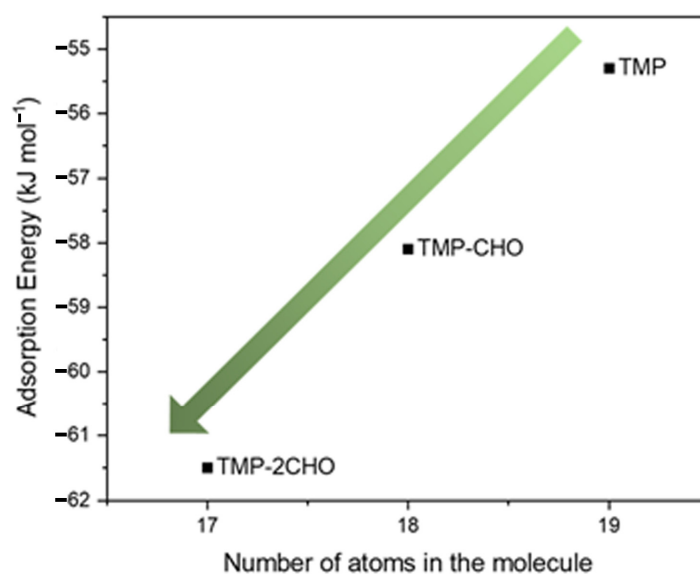


Figure 8. Adsorption energies for TMP, TMP-CHO, and TMP-2CHO on the pristine graphene surface versus the number of atoms in the molecule.

3. Materials and Methods

The specific initial geometries of volatile organic compounds near graphene layer were obtained after molecular mechanics and molecular dynamics simulations using a simulation protocol adopted in previous work [90] about the adsorption process on graphite, graphene surface. These data will be published in a future paper related to the adsorption of single volatile compounds on graphene surface and at larger concentration.

Optimal adsorption configurations were derived using pw.x software, part of the Quantum ESPRESSO suite of codes [92]. This package is widely used to simulate the behavior of materials and molecules, and pw.x software [93] specifically performs Density Functional theory (DFT) calculations related to the electronic structures of materials. A non-empirical generalized gradient approximation functional, namely, Perdew–Burke–Ernzerhof (PBE), was used [94], and standard solid-state ultrasoft pseudopotentials were employed to process the electron–ion interactions for all the atoms [95]. The kinetic energy cutoff of the plane wave basis set was fixed at 60 Ryd. For pristine graphene systems, a $3 \times 3 \times 1$ Monkhorst–Pack set was used to sample the Brillouin zones, while the other simulations were performed at the Γ point. To account for dispersion (Van der Waals) interactions, which, as mentioned in the introduction, are important in describing physisorption on graphene-based systems, the “DFT-D of Grimme” algorithm was used [96].

To model the pristine graphene sheet, a periodic unit cell with dimensions of $6 \times 5 \times 1$ was built. The unit cell contained 60 carbon atoms, and the lattice parameters were set to 12.30 Å, 12.78 Å, and 20.33 Å in the a, b, and c directions, respectively. To prevent any interaction that could introduce errors in the analysis, the c parameter (the height of the box in which the calculation was carried out) was adjusted to 20 Å, ensuring a sufficient separation between the graphene layers.

Regarding the different types of small organic molecules adsorbed on the surface of graphene, the analyzed compounds and their chemical structures are listed in Table 1. For the R group, linear alkyl chains were investigated by increasing the number of carbon atoms from methane to butane; the other molecules were cyclic saturated with cyclopentane, pyrrolidine, unsaturated cyclic cyclopentadiene, and pyrrole.

With regard to adsorption energy, it is important to highlight that to quantify the interaction force between the adsorbate and the investigated surface, adsorption energy (E_{ads}) was calculated as follows:

$$E_{ads} = E_{(S+A)} - E_A - E_S$$

Above, $E_{(S+A)}$ is the total energy of the adsorbate/surface system, E_A is the total energy of the molecule calculated with the same cell and electronic parameters of the whole system, and E_S is the total energy of the investigated surface. As a quantity strictly connected to the thermodynamics of adsorption, the more negative the value, the more favorable the process.

Charge density difference plots were used to visualize the charge transfer and charge disequilibria between atoms from the adsorbate, and surface charge density difference (CDD) maps were calculated using the pp.x software contained in the Quantum ESPRESSO Suite. $\Delta\rho$ was calculated using the following formula:

$$\Delta\rho = \rho_{(S+A)} - \rho_A - \rho_S$$

Above, $\rho_{(S+A)}$ is the charge density of the adsorbate/surface system, ρ_A is the charge density of the molecule (calculated with the same cell and electronic parameters of the whole system), and ρ_S is the charge density of the investigated surface. Following this methodology, $\Delta\rho$ (or, more specifically, its iso-surface) shows the variations in the charge density of the graphene–adsorbate system. In the figures, a difference in charge density is shown in red on an iso-surface on which the accumulation of charge is represented, while blue indicates depletion [97,98].

4. Conclusions

The DFT study of pyrroles and pyrrole derivatives adsorbed on graphene surface revealed that adsorption process is predominantly governed by dispersion forces and π – π bonding interactions. The number of atoms in the molecules considered and the presence of π electrons significantly influence the corresponding adsorption energy. A linear dependence of the adsorption energy is found as a function of the number of atoms in the adsorbed molecules. The pyrrole compounds display more favorable supramolecular interactions with graphene surface. In particular, at the same number of atoms in contact with the graphene surface pyrroles and cyclopentadienes are 10 kJ mol^{-1} more stable than the corresponding unsaturated ones. Furthermore, the presence of aldehydic groups in pyrrole derivatives improves the adsorption energy which is therefore more negative. This study provides valuable insights into supramolecular interactions and their influence on the first step of the adsorption process, contributing to the fundamental understanding of surface modifications for carbon allotropes and their applications in polymer composites.

Overall, the findings of this study offer valuable insights into the complex mechanisms governing adsorption on carbon allotrope surfaces. By elucidating the significant roles of dispersion forces and π – π bonding interactions, this research study contributes to a comprehensive understanding of surface modifications for carbon allotropes and their potential applications in the field of polymer composites. Further study on the adsorption process of these molecules on the graphene surface as single molecules and at higher concentrations will be performed using molecular mechanics and molecular dynamics methods to better understand the contribution of van der Waals interactions in the adsorption process in a more complex supramolecular structure as in previous work [90].

Author Contributions: Conceptualization, M.G. and G.R.; methodology, F.M. and G.R.; software, F.M. and G.R.; validation, F.M., V.B., M.G. and G.R.; formal analysis, F.M. and G.R.; investigation, F.M. and G.R.; resources, F.M., V.B., M.G. and G.R.; data curation, F.M. and G.R.; writing—original draft preparation, F.M. and G.R.; writing—review and editing, F.M., V.B., M.G. and G.R.; visualization, G.R.; supervision, M.G. and G.R.; project administration, M.G. and G.R.; funding acquisition, M.G. and G.R. All authors have read and agreed to the published version of the manuscript.

Funding: This research was funded by Made in Italy–Circular and Sustainable (MICS) Extended Partnership funded by the European Union Next-Generation EU (Piano Nazionale di Ripresa e Resilienza (PNRR)–Missione 4, Componente 2, Investimento 1.3–D.D. 1551.11-10-2022, PE00000004) for financial support. This research was also funded by ICSC—Centro Nazionale di Ricerca in High Performance Computing, Big Data, and Quantum Computing funded by European Union—NextGenerationEU. F.M., V.B. and M.G. gratefully acknowledge BIRLA Carbon for funding the research.

Data Availability Statement: Data are contained within the article.

Acknowledgments: The authors acknowledge CINECA HPC clusters (grant HP10CKOQOB) for the computational resources.

Conflicts of Interest: The authors declare no conflict of interest.

References

1. Magne, T.M.; Vieira, T.D.; Alencar, L.M.R.; Maia, F.F.M.; Gemini-Piperni, S.; Carneiro, S.V.; Fechine, L.M.U.D.; Freire, R.M.; Golokhvast, K.; Metrangolo, P.; et al. Graphene and its derivatives: Understanding the main chemical and medicinal chemistry roles for biomedical applications. *J. Nanostructure Chem.* **2022**, *12*, 693–727. [[CrossRef](#)]
2. Criado, A.; Melchionna, M.; Marchesan, S.; Prato, M. The Covalent Functionalization of Graphene on Substrates. *Angew. Chem. Int. Ed.* **2015**, *54*, 10734–10750. [[CrossRef](#)] [[PubMed](#)]
3. Park, W.; Shin, H.; Choi, B.; Rhim, W.K.; Na, K.; Keun Han, D. Advanced hybrid nanomaterials for biomedical applications. *Prog. Mater. Sci.* **2020**, *114*, 1–110.
4. Liu, S. Cooperative adsorption on solid surfaces. *J. Colloid Interface Sci.* **2015**, *450*, 224. [[CrossRef](#)]
5. Freund, H.J. Adsorption of gases on complex: Solid surfaces. *Angew. Chem. Int. Ed.* **1997**, *36*, 452. [[CrossRef](#)]
6. Carr, A.J.; Carr, A.; Lee, S.E.; Uysal, A. Ion and water adsorption to graphene and graphene oxide surfaces. *Nanoscale* **2023**, *15*, 14319. [[CrossRef](#)]
7. Krishna, R.H.; Chandraprabha, M.N.; Samrat, K.; Murthy, T.P.K.; Manjunatha, C.; Kumar, S.G. Carbon nanotubes and graphene-based materials for adsorptive removal of metal ions—A review on surface functionalization and related adsorption mechanism. *Appl. Surf. Sci. Adv.* **2023**, *16*, 100431.
8. Yang, G.; Li, L.; Lee, W.B.; Ng, M.C. Structure of Graphene and Its Disorders: A Review. *Sci. Technol. Adv. Mater.* **2018**, *19*, 613–648. [[CrossRef](#)]
9. Liu, Y.; Ge, Z.; Li, Z.; Chen, Y. High-power instant-synthesis technology of carbon nanomaterials and nanocomposites. *Nano Energy* **2021**, *80*, 1–61.
10. Ali, I.; Pakharukov, Y.; Shabiev, F.K.; Galunin, E.; Safargaliev, R.F.; Vasiljev, S.A.; Ezdin, B.S.; Burakov, A.E.; Alothman, Z.A.; Sillanpaa, M. Preparation of graphene based nanofluids: Rheology determination and theoretical analysis of the molecular interactions of graphene nanoparticles. *J. Mol. Liq.* **2023**, *390*, 122954. [[CrossRef](#)]
11. Old 6 Bahiraei, M.; Heshmatian, S. Graphene family nanofluids: A critical review and future research directions. *Energy Convers. Manag.* **2019**, *196*, 1222–1256. [[CrossRef](#)]
12. Kumar, K.V.; Gadipelli, S.; Wood, B.; Ramisetty, K.A.; Stewart, A.A.; Howard, C.A.; Brett, D.J.L.; Rodriguez-Reinoso, F. Characterization of the adsorption site energies and heterogeneous surfaces of porous materials. *J. Mater. Chem. A* **2019**, *7*, 10104. [[CrossRef](#)]
13. Lin, L.C.; Thirumavalavan, M.; Wang, Y.T.; Lee, J.F. Surface area and pore size tailoring of mesoporous silica materials by different hydrothermal treatments and adsorption of heavy metal ions. *Colloids Surf. A Physicochem. Eng. Asp.* **2010**, *319*, 223. [[CrossRef](#)]
14. Dong, D.M.; Hua, X.Y.; Li, Y.; Li, Z.H. Lead adsorption to metal oxides and organic material of freshwater surface coatings determined using a novel selective extraction method. *Environ. Pollut.* **2002**, *119*, 317. [[CrossRef](#)]
15. Zhang, W.; Wu, C.M.; Li, Y.R. Determination of the surface properties and adsorption states of nanoporous materials using the zeta adsorption isotherm. *Phys. Chem. Chem. Phys.* **2023**, *25*, 22669. [[CrossRef](#)]
16. Mao, K.; Gao, L.S.; Lv, X.C.; Gao, D.D.; Lv, J.Z.; Bai, M.L. Numerical simulation of forced convection heat transfer mechanism and comprehensive performance on hydrophobic structure surface. *Int. J. Therm. Sci.* **2023**, *184*, 107895. [[CrossRef](#)]
17. Kubota, T.; Watanabe, N.; Ohtsuka, S.; Iwasaki, T.; Ono, K.; Iriye, Y.; Samukawa, S. Numerical simulation on neutral beam generation mechanism by collision of positive and negative chlorine ions with graphite surface. *J. Phys. D Appl. Phys.* **2011**, *44*, 125203. [[CrossRef](#)]
18. Zhao, D.; Liu, X.Q. Study on the microscopic mechanism of adsorption and diffusion of hydrocarbon oil drops on coal surface using molecular dynamics simulations. *Int. J. Quantum. Chem.* **2023**, *123*, e27229. [[CrossRef](#)]
19. Zhao, L.F.; Liu, W.L.; Shen, Y.Z.; Xu, Y.J.S.; Jiang, B.; Tao, J. Ice adhesion mechanism on the patterned surface of aluminum matrix and array graphene based on molecular dynamics simulations. *Appl. Phys. Lett.* **2023**, *123*, 061602. [[CrossRef](#)]
20. James, J.N.; Sholl, D.S. Theoretical studies of chiral adsorption on solid surfaces. *J. Colloid Interface Sci.* **2008**, *13*, 60. [[CrossRef](#)]
21. Amrhar, O.; Lee, H.S.; Lgaz, H.; Berisha, A.; Ebenso, E.E.; Cho, Y.J. Computational insights into the adsorption mechanisms of anionic dyes on the rutile TiO₂ (110) surface: Combining SCC-DFT tight binding with quantum chemical and molecular dynamics simulations. *J. Mol. Liq.* **2023**, *377*, 121554. [[CrossRef](#)]
22. Dehmani, Y.; Lgaz, H.; Alrashdi, A.A.; Lamhasni, T.; Abouarnadasse, S.; Chung, I.M. Phenol adsorption mechanism on the zinc oxide surface: Experimental, cluster DFT calculations, and molecular dynamics simulations. *J. Mol. Liq.* **2021**, *324*, 114993. [[CrossRef](#)]
23. Yi, P.; Zuo, X.Z.; Lang, D.; Wu, M.; Dong, W.; Chen, Q.; Zhang, L.J. Competitive adsorption of methanol co-solvent and dioctyl phthalate on functionalized graphene sheet: Integrated investigation by molecular dynamics simulations and quantum chemical calculations. *J. Colloid Interface Sci.* **2021**, *605*, 354. [[CrossRef](#)] [[PubMed](#)]

24. Tang, H.; Zhang, S.Y.; Huang, T.L.; Cui, F.Y.; Xing, B.S. pH-Dependent adsorption of aromatic compounds on graphene oxide: An experimental, molecular dynamics simulation and density functional theory investigation. *J. Hazard. Mater.* **2020**, *395*, 122680. [[CrossRef](#)] [[PubMed](#)]
25. Sun, C.Z.; Liu, M.; Bai, B.F. Molecular simulations on graphene-based membranes. *Carbon* **2019**, *153*, 481–494. [[CrossRef](#)]
26. Qiu, Z.Y.; Li, P.; Li, Z.Y.; Yang, J.L. Atomistic Simulations of Graphene Growth: From Kinetics to Mechanism. *Acc. Chem. Res.* **2018**, *51*, 728–735. [[CrossRef](#)]
27. Ganazzoli, F.; Raffaini, G. Classical atomistic simulations of protein adsorption on carbon nanomaterials. *Curr. Opin. Colloid Interface Sci.* **2019**, *41*, 11–26. [[CrossRef](#)]
28. Yang, J.; Yang, X.N.; Li, Y.P. Molecular simulation perspective of liquid-phase exfoliation, dispersion, and stabilization for graphene. *Curr. Opin. Colloid Interface Sci.* **2015**, *20*, 339–345. [[CrossRef](#)]
29. Thapa, R.; Ugwumadu, C.; Nepal, K.; Trembly, J.; Drabold, D.A. Ab Initio Simulation of Amorphous Graphite. *Phys. Rev. Lett.* **2022**, *128*, 236402. [[CrossRef](#)]
30. Cutini, M.; Civalleri, B.; Corno, M.; Orlando, R.; Brandenburg, J.G.; Maschio, L.; Ugliengo, P. Assessment of Different Quantum Mechanical Methods for the Prediction of Structure and Cohesive Energy of Molecular Crystals. *J. Chem. Theory Comput.* **2016**, *12*, 3340. [[CrossRef](#)]
31. Brann, M.R.; Ma, X.Y.; Sibener, S.J. Isotopic Enrichment Resulting from Differential Condensation of Methane Isotopologues Involving Non-equilibrium Gas-Surface Collisions Modeled with Molecular Dynamics Simulations. *J. Phys. Chem. C* **2023**, *127*, 13286–13294. [[CrossRef](#)]
32. Jiang, M.M.; Zhang, C.; Liao, N.B.; Zhao, T.C.; Ge, J.Q. Self-cantilever phenomenon of graphite/graphenes micro/nano structure: Experiment and DFT simulation analysis. *Appl. Surf. Sci.* **2021**, *545*, 149009. [[CrossRef](#)]
33. Raffaini, G.; Catauro, M. Surface Interactions between Ketoprofen and Silica-Based Biomaterials as Drug Delivery System Synthesized. Sol-Gel: A Molecular Dynamics Study. *Materials* **2022**, *15*, 2759. [[CrossRef](#)]
34. Catauro, M.; Barrino, F.; Dal Poggetto, G.; Milazzo, M.; Blanco, I.; Cipriotti, S.V. Structure, drug absorption, bioactive and antibacterial properties of sol-gel SiO₂/ZrO₂ materials. *Ceram. Int.* **2020**, *46*, 29459. [[CrossRef](#)]
35. Johnson, R.P.; Jeong, Y.I.; Choi, E.; Chung, C.W.; Kang, D.H.; Oh, S.O.; Suh, H.; Kim, I. Biocompatible Poly(2-hydroxyethyl methacrylate)-b-poly(L-histidine) Hybrid Materials for pH-Sensitive Intracellular Anticancer Drug Delivery. *Adv. Funct. Mater.* **2012**, *22*, 1058. [[CrossRef](#)]
36. Xie, Y.H.; Kong, Y.; Gao, H.J.; Soh, A.K. Molecular dynamics simulation of polarizable carbon nanotubes. *Comput. Mater. Sci.* **2007**, *40*, 460–465. [[CrossRef](#)]
37. Li, J.; Liu, Q.H.; Flores, R.A.; Lemmon, J.; Bligaard, T. DFT simulation of the X-ray diffraction pattern of aluminum-ion-intercalated graphite used as the cathode material of the aluminum-ion battery. *Phys. Chem. Chem. Phys.* **2020**, *22*, 5969–5975. [[CrossRef](#)]
38. Pal, G.; Kumar, S. Modeling of carbon nanotubes and carbon nanotube-polymer composites. *Prog. Aerosp. Sci.* **2016**, *80*, 33–58. [[CrossRef](#)]
39. Raffaini, G.; Elli, S.; Ganazzoli, F. Computer simulation of bulk mechanical properties and surface hydration of biomaterials. *J. Biomed. Mater. Res. A* **2006**, *77A*, 618–626. [[CrossRef](#)]
40. Guo, W.M.; Bai, Q.S.; Dou, Y.H.; Wang, H.F.; Chen, S.D. Molecular Dynamics Study on the Effects of Substrate Grain Boundaries on the Adsorption State of Graphene: Implications for Nanoscale Lubrication. *ACS Appl. Nano Mater.* **2023**, *6*, 8093. [[CrossRef](#)]
41. Li, Q.L.; Zhu, S.M.; Hao, G.Z.; Hu, Y.B.; Wu, F.; Jiang, W. Fabrication of thermoresponsive metal-organic nanotube sponge and its application on the adsorption of endocrine-disrupting compounds and pharmaceuticals/personal care products: Experiment and molecular simulation study. *Environ. Pollut.* **2021**, *273*, 116466. [[CrossRef](#)]
42. Salehi, A.; Rash-Ahmadi, S. Effect of adsorption, hardener, and temperature on mechanical properties of epoxy nanocomposites with functionalized graphene: A molecular dynamics study. *J. Mol. Graph. Model.* **2022**, *117*, 108311. [[CrossRef](#)]
43. Mantero, S.; Piuri, D.; Montecchi, F.M.; Vesentini, S.; Ganazzoli, F.; Raffaini, G. Albumin adsorption onto pyrolytic carbon: A molecular mechanics approach. *J. Biomed. Mater. Res.* **2002**, *59*, 329–339. [[CrossRef](#)]
44. Li, B.; Mi, C.W. Atomistic insights on the adsorption of long-chain undecane molecules on carbon nanotubes: Roles of chirality and surface hydroxylation. *Diam. Relat. Mater.* **2023**, *133*, 109706. [[CrossRef](#)]
45. Taheri, Z.; Pour, A.N. Studying of the adsorption and diffusion behaviors of methane on graphene oxide by molecular dynamics simulation. *J. Mol. Model.* **2021**, *27*, 59. [[CrossRef](#)] [[PubMed](#)]
46. Comer, J.; Chen, R.; Poblete, H.; Vergara-Jaque, A.; Riviere, J.E. Predicting Adsorption Affinities of Small Molecules on Carbon Nanotubes Using Molecular Dynamics Simulation. *ACS Nano* **2015**, *9*, 11761–11774. [[CrossRef](#)] [[PubMed](#)]
47. Raffaini, G.; Ganazzoli, F. Separation of chiral nanotubes with an opposite handedness by chiral oligopeptide adsorption: A molecular dynamics study. *J. Chromatogr. A* **2016**, *1425*, 221–230. [[CrossRef](#)] [[PubMed](#)]
48. Barinov, N.A.; Prokhorov, V.V.; Dubrovin, E.V.; Klinov, D.V. AFM visualization at a single-molecule level of denaturated states of proteins on graphite. *Colloids Surf. B-Biointerfaces* **2016**, *146*, 777–784. [[CrossRef](#)]
49. Karajanagi, S.S.; Yang, H.C.; Asuri, P.; Sellitto, E.; Dordick, J.S.; Kane, R.S. Protein-assisted solubilization of single-walled carbon nanotubes. *Langmuir* **2006**, *22*, 1392–1395. [[CrossRef](#)]
50. Hasnip, P.J.; Refson, K.; Probert, M.I.; Yates, J.R.; Clark, S.J.; Pickard, C.J. Density Functional Theory in the Solid State. *Philos. Trans. R. Soc. A Math. Phys. Eng. Sci.* **2014**, *372*. [[CrossRef](#)]

51. Ostovari, F.; Hasanpoori, M.; Abbasnejad, M.; Saleh, M.A. DFT calculations of graphene monolayer in presence of Fe dopant and vacancy. *Phys. B Condens. Matter*. **2018**, *541*, 6–13. [[CrossRef](#)]
52. Gecim, G.; Ozekmekci, M. A density functional theory study of molecular H₂S adsorption on (4,0) SWCNT doped with Ge, Ga and B. *Surf. Sci.* **2021**, *711*, 121876. [[CrossRef](#)]
53. Kamedulski, P.; Kaczmarek-Kedziera, A.; Lukaszewicz, J. Influence of intermolecular interactions on the properties of carbon nanotubes. *Bull. Mater. Sci* **2018**, *41*, 76. [[CrossRef](#)]
54. Lejaeghere, K.; Bihlmayer, G.; Björkman, T.; Blaha, P.; Blügel, S.; Blum, V.; Caliste, D.; Castelli, I.E.; Clark, S.J.; Dal Corso, A.; et al. Reproducibility in Density Functional Theory Calculations of Solids. *Science* **2016**, *351*, aad3000. [[CrossRef](#)]
55. Mittal, G.; Dhand, V.; Rhee, K.Y.; Park, S.J.; Lee, W.R. A Review on Carbon Nanotubes and Graphene as Fillers in Reinforced Polymer Nanocomposites. *J. Ind. Eng. Chem.* **2015**, *21*, 11–25. [[CrossRef](#)]
56. Al-Hartomy, O.A.; Al-Ghamdi, A.A.; Al-Salamy, F.; Dishovsky, N.; Slavcheva, D.; El-Tantawy, F. Properties of Natural Rubber-Based Composites Containing Fullerene. *Int. J. Polym. Sci.* **2012**, *2012*, 967276. [[CrossRef](#)]
57. Khuntawee, W.; Sutthibutpong, T.; Phongphanphanee, S.; Karttunen, M.; Wong-ekkabut, J. Molecular dynamics study of natural rubber-fullerene composites: Connecting microscopic properties to macroscopic behavior. *Phys. Chem. Chem. Phys.* **2019**, *21*, 19403–19413. [[CrossRef](#)] [[PubMed](#)]
58. Kitjanon, J.; Khuntawee, W.; Phongphanphanee, S.; Sutthibutpong, T.; Chattham, N.; Karttunen, M.; Wong-ekkabut, J. Nanocomposite of Fullerenes and Natural Rubbers: MARTINI Force Field Molecular Dynamics Simulations. *Polymers* **2021**, *13*, 4044. [[CrossRef](#)]
59. Rong, M.Z.; Zhang, M.Q.; Ruan, W.H. Surface Modification of Nanoscale Fillers for Improving Properties of Polymer Nanocomposites: A Review. *Mater. Sci. Technol.* **2006**, *22*, 787–796. [[CrossRef](#)]
60. Shen, X.; Wang, Z.; Wu, Y.; Liu, X.; Kim, J.K. Effect of Functionalization on Thermal Conductivities of Graphene/Epoxy Composites. *Carbon N. Y.* **2016**, *108*, 412–422. [[CrossRef](#)]
61. Patti, A.; Russo, P.; Acierno, D.; Acierno, S. The Effect of Filler Functionalization on Dispersion and Thermal Conductivity of Polypropylene/Multi Wall Carbon Nanotubes Composites. *Compos. Part B Eng.* **2016**, *94*, 350–359. [[CrossRef](#)]
62. Shen, C.; Oyadiji, S.O. The Processing and Analysis of Graphene and the Strength Enhancement Effect of Graphene-Based Filler Materials: A Review. *Mater. Today Phys.* **2020**, *15*, 100257. [[CrossRef](#)]
63. Tang, B.; Hu, G.; Gao, H.; Hai, L. Application of Graphene as Filler to Improve Thermal Transport Property of Epoxy Resin for Thermal Interface Materials. *Int. J. Heat Mass Transf.* **2015**, *85*, 420–429. [[CrossRef](#)]
64. Zhou, Z.; Wang, S.; Zhang, Y.; Zhang, Y. Effect of Different Carbon Fillers on the Properties of PP Composites: Comparison of Carbon Black with Multiwalled Carbon Nanotubes. *J. Appl. Polym. Sci.* **2006**, *102*, 4823–4830. [[CrossRef](#)]
65. Kwon, Y.J.; Park, J.B.; Jeon, Y.P.; Hong, J.Y.; Park, H.S.; Lee, J.U. A Review of Polymer Composites Based on Carbon Fillers for Thermal Management Applications: Design, Preparation, and Properties. *Polymers* **2021**, *13*, 1312. [[CrossRef](#)]
66. Kim, H.; Abdala, A.A.; MacOsco, C.W. Graphene/Polymer Nanocomposites. *Macromolecules* **2010**, *43*, 6515–6530. [[CrossRef](#)]
67. Dai, J.-F.; Wang, G.-J.; Ma, L.; Wu, C.-K.; Wang, G.-J.; Dai, J.-F.; Wang, G.-J.; Ma, L.; Wu, C.-K. Surface Properties of Graphene: Relationship to Graphene-Polymer composites. *Rev. Adv. Mater. Sci.* **2015**, *40*, 60–71.
68. Cadek, M.; Coleman, J.N.; Ryan, K.P.; Nicolosi, V.; Bister, G.; Fonseca, A.; Nagy, J.B.; Szostak, K.; Béguin, F.; Blau, W.J. Reinforcement of Polymers with Carbon Nanotubes: The Role of Nanotube Surface Area. *Nano Lett.* **2004**, *4*, 353–356. [[CrossRef](#)]
69. Kim, S.W.; Kim, T.; Kim, Y.S.; Choi, H.S.; Lim, H.J.; Yang, S.J.; Park, C.R. Surface modifications for the effective dispersion of carbon nanotubes in solvents and polymers. *Carbon* **2012**, *50*, 3–33. [[CrossRef](#)]
70. Eitan, A.; Jiang, K.Y.; Dukes, D.; Andrews, R.; Schadler, L.S. Surface modification of multiwalled carbon nanotubes: Toward the tailoring of the interface in polymer composites. *Chem. Mater.* **2003**, *15*, 3198–3201. [[CrossRef](#)]
71. Zhao, W.; Song, C.H.; Pehrsson, P.E. Water-soluble and optically pH-sensitive single-walled carbon nanotubes from surface modification. *J. Am. Chem. Soc.* **2002**, *124*, 12418–12419. [[CrossRef](#)] [[PubMed](#)]
72. Sun, J.T.; Hong, C.Y.; Pan, C.Y. Surface modification of carbon nanotubes with dendrimers or hyperbranched polymers. *Polym. Chem.* **2011**, *2*, 998. [[CrossRef](#)]
73. Verma, B.; Balomajumder, C. Surface modification of one-dimensional Carbon Nanotubes: A review for the management of heavy metals in wastewater. *Environ. Technol. Innov.* **2020**, *17*, 100596. [[CrossRef](#)]
74. Atif, M.; Afzaal, I.; Naseer, H.; Abrar, M.; Bongiovanni, R. Review-Surface Modification of Carbon Nanotubes: A Tool to Control Electrochemical Performance. *ECS J. Solid State Sci. Technol.* **2020**, *9*, 041009. [[CrossRef](#)]
75. Barbera, V.; Bernardi, A.; Palazzolo, A.; Rosengart, A.; Brambilla, L.; Galimberti, M. Facile and Sustainable Functionalization of Graphene Layers with Pyrrole Compounds. *Pure Appl. Chem.* **2018**, *90*, 253–270. [[CrossRef](#)]
76. Galimberti, M.; Barbera, V.; Guerra, S.; Conzatti, L.; Castiglioni, C.; Brambilla, L.; Serafini, A. Biobased Janus Molecule for the Facile Preparation of Water Solutions of Few Layer Graphene Sheets. *RSC Adv.* **2015**, *5*, 81142–81152. [[CrossRef](#)]
77. Barbera, V.; Brambilla, L.; Milani, A.; Palazzolo, A.; Castiglioni, C.; Vitale, A.; Bongiovanni, R.; Galimberti, M. Domino Reaction for the Sustainable Functionalization of Few-Layer Graphene. *Nanomaterials* **2019**, *9*, 44. [[CrossRef](#)]
78. Galimberti, M.; Barbera, V.; Citterio, A.; Sebastiano, R.; Truscello, A.; Valerio, A.M.; Conzatti, L.; Mendichi, R. Supramolecular Interactions of Carbon Nanotubes with Biosourced Polyurethanes from 2-(2,5-Dimethyl-1H-Pyrrol-1-Yl)-1,3-Propanediol. *Polymer* **2015**, *63*, 62–70. [[CrossRef](#)]

79. Prioglio, G.; Agnelli, S.; Conzatti, L.; Balasooriya, W.; Schritteser, B.; Galimberti, M. Graphene Layers Functionalized with a Janus Pyrrole-Based Compound in Natural Rubber Nanocomposites with Improved Ultimate and Fracture Properties. *Polymers* **2020**, *12*, 944. [[CrossRef](#)]
80. Dindorkar, S.S.; Sinha, N.; Yadav, A. Comparative Study on Adsorption of Volatile Organic Compounds on Graphene, Boron Nitride and Boron Carbon Nitride Nanosheets. *Solid State Commun.* **2023**, *359*, 115021. [[CrossRef](#)]
81. Lazar, P.; Karlický, F.; Jurecka, P.; Kocman, M.; Otyepková, E.; Šafářová, K.; Otyepka, M. Adsorption of Small Organic Molecules on Graphene. *J. Am. Chem. Soc.* **2013**, *135*, 6372–6377. [[CrossRef](#)] [[PubMed](#)]
82. Lee, J.; Min, K.A.; Hong, S.; Kim, G. Ab Initio Study of Adsorption Properties of Hazardous Organic Molecules on Graphene: Phenol, Phenyl Azide, and Phenylnitrene. *Chem. Phys. Lett.* **2015**, *618*, 57–62. [[CrossRef](#)]
83. Xu, H.; Guan, D.; Ma, L. The bio-inspired heterogeneous single-cluster catalyst Ni₁₀₀-Fe₄S₄ for enhanced electrochemical CO₂ reduction to CH₄. *Nanoscale* **2023**, *15*, 2756. [[CrossRef](#)] [[PubMed](#)]
84. Knorr, L. Einwirkung des Diacetbernsteinsäureesters auf Ammoniak und primäre Aminbasen. *Chem. Ber.* **1885**, *18*, 299. [[CrossRef](#)]
85. Paal, C. Synthese von Thiophen- und Pyrrolderivaten. *Chem. Ber.* **1885**, *18*, 367. [[CrossRef](#)]
86. Barbera, V.; Galimberti, M.; Giannini, L.; Naddeo, S. Process for the Preparation of Diketones and Pyrrole Derivatives. Patent Application n. PCT/IB2022/062453, 19 December 2022.
87. Prioglio, G.; Naddeo, S.; Giese, U.; Barbera, V.; Galimberti, M. Bio-Based Pyrrole Compounds Containing Sulfur Atoms as Coupling Agents of Carbon Black with Unsaturated Elastomers. *Nanomaterials* **2023**, *13*, 2761. [[CrossRef](#)]
88. Magaletti, F.; Margani, F.; Monti, A.; Dezyani, R.; Prioglio, G.; Giese, U.; Barbera, V.; Galimberti, M.S. Adducts of Carbon Black with a Biosourced Janus Molecule for Elastomeric Composites with Lower Dissipation of Energy. *Polymers* **2023**, *15*, 3120. [[CrossRef](#)]
89. Pirelli Tyre; Annual Report: The Human Dimension. 2020, 106. Available online: https://corporate.pirelli.com/var/files2020/EN/PDF/PIRELLI_ANNUAL_REPORT_2020_ENG.pdf (accessed on 4 October 2022).
90. Raffaini, G.; Ganazzoli, F. Surface topography effects in protein adsorption on nanostructured carbon allotropes. *Langmuir*. **2013**, *29*, 4883. [[CrossRef](#)]
91. Barbera, V.; Brambilla, L.; Porta, A.; Bongiovanni, R.; Vitale, A.; Torrisi, G.; Galimberti, M. Selective Edge Functionalization of Graphene Layers with Oxygenated Groups by Means of Reimer-Tiemann and Domino Reimer-Tiemann/Cannizzaro Reactions. *J. Mater. Chem. A* **2018**, *6*, 7749–7761. [[CrossRef](#)]
92. Giannozzi, P.; Baroni, S.; Bonini, N.; Calandra, M.; Car, R.; Cavazzoni, C.; Ceresoli, D.; Chiarotti, G.L.; Cococcioni, M.; Dabo, I.; et al. QUANTUM ESPRESSO: A Modular and Open-Source Software Project for Quantum Simulations of Materials. *J. Phys. Condens. Matter* **2009**, *21*, 395502. [[CrossRef](#)]
93. QuantumEspresso PWscf User's Guide (v.7.2). Available online: https://www.quantum-espresso.org/Doc/pw_user_guide/ (accessed on 4 October 2022).
94. Perdew, J.P.; Burke, K.; Ernzerhof, M. Generalized Gradient Approximation Made Simple. *Phys. Rev. Lett.* **1996**, *77*, 3865–3868. [[CrossRef](#)] [[PubMed](#)]
95. Prandini, G.; Marrazzo, A.; Castelli, I.E.; Mounet, N.; Marzari, N. Precision and Efficiency in Solid-State Pseudopotential Calculations. *NPJ Comput. Mater.* **2018**, *4*, 72. [[CrossRef](#)]
96. Grimme, S.; Antony, J.; Ehrlich, S.; Krieg, H. A Consistent and Accurate Ab Initio Parametrization of Density Functional Dispersion Correction (DFT-D) for the 94 Elements H-Pu. *J. Chem. Phys.* **2010**, *132*. [[CrossRef](#)] [[PubMed](#)]
97. Zhuoran, L.; Xu, H.; Xu, W.; Peng, B.; Zhao, C.; Xie, M.; Lv, X.; Gao, Y.; Hu, K.; Fang, Y.; et al. Quasi-Topological Intercalation Mechanism of Bi_{0.67}NbS₂ Enabling 100 C Fast-Charging for Sodium-Ion Batteries. *Adv. Energy Mater.* **2023**, *13*, 202300790.
98. Xiao, W.; Kiran, G.K.; Yoo, K.; Kim, J.H.; Xu, H. The Dual-Site Adsorption and High Redox Activity Enabled by Hybrid Organic-Inorganic Vanadyl Ethylene Glycolate for High-Rate and Long-Durability Lithium–Sulfur Batteries. *Small* **2023**, *19*, 202206750. [[CrossRef](#)]

Disclaimer/Publisher's Note: The statements, opinions and data contained in all publications are solely those of the individual author(s) and contributor(s) and not of MDPI and/or the editor(s). MDPI and/or the editor(s) disclaim responsibility for any injury to people or property resulting from any ideas, methods, instructions or products referred to in the content.